

# Nephroprotective effect of pioglitazone in a Wistar rat model of adenine-induced chronic kidney disease

MARIANA CECILIA PÉREZ-VILLALOBOS<sup>1</sup>, ANDREA BARBA-GONZÁLEZ<sup>1</sup>, NICTÉ GARCÍA-CARRILLO<sup>1</sup>,  
MARTÍN HUMBERTO MUÑOZ-ORTEGA<sup>2</sup>, ESPERANZA SÁNCHEZ-ALEMÁN<sup>1,3</sup>,  
MANUEL ENRIQUE ÁVILA-BLANCO<sup>1</sup>, JORGE CHRISTOPHER MORONES-GAMBOA<sup>1</sup>,  
JAVIER VENTURA-JUÁREZ<sup>1</sup> and SANDRA LUZ MARTÍNEZ-HERNÁNDEZ<sup>4</sup>

<sup>1</sup>Department of Morphology, Center of Basic Sciences, Autonomous University of Aguascalientes, 20100 Aguascalientes, Mexico;

<sup>2</sup>Department of Chemistry, Center of Basic Sciences, Autonomous University of Aguascalientes, 20100 Aguascalientes, Mexico;

<sup>3</sup>Family Medicine Unit 8, Mexican Social Security Institute, 20180 Aguascalientes, Mexico; <sup>4</sup>Department of Microbiology, Center of Basic Sciences, Autonomous University of Aguascalientes, 20100 Aguascalientes, Mexico

Received March 5, 2024; Accepted June 27, 2024

DOI: 10.3892/etm.2024.12681

**Abstract.** Chronic kidney disease (CKD) is a progressive disease with a high mortality rate and a worldwide prevalence of 13.4%, triggered by various diseases with high incidence. The aim of the present study was to investigate the anti-inflammatory and antifibrotic effect of pioglitazone on kidney in an adenine-induced Wistar rats and the mechanisms possibly involved. CKD was induced in 40 rats. Rats were divided into two groups, which were split into the following sub-groups: i) Therapeutic (pioglitazone administered after renal damage) divided into intact (healthy), adenine (CKD) and adenine/pioglitazone (treatment) and ii) prophylactic (adenine and pioglitazone administered at the same time) split into intact (healthy), adenine (CKD), endogenous reversion (recovery without treatment), adenine/pioglitazone (treatment) and pioglitazone sub-groups. Reverse transcription-quantitative PCR (collagen I,  $\alpha$ -SMA and TGF- $\beta$ ), and hematoxylin-eosin, Masson's trichrome and Sirius red staining were performed to measure histological markers of kidney damage, also the serum markers (urea, creatinine and uric acid) were performed, for analyze the effects of pioglitazone. In the adenine/pioglitazone rats of the therapeutic group, renal function parameters

such as eGFR increased and serum creatinine decreased from those of untreated rats (CKD), however the renal index, serum urea, abnormalities in renal morphology, inflammatory cells and relative gene expression of collagen I,  $\alpha$ -SMA and TGF- $\beta$  did not change relative to the CKD rats. In adenine/pioglitazone rats, extracellular matrix collagen accumulation was significantly lower than the CKD rats. On the other hand, in adenine/pioglitazone rats of the prophylactic group, the renal index, creatinine, urea, uric acid serum and relative gene expression of collagen I,  $\alpha$ -SMA, and TGF- $\beta$  were significantly lower, as well as the presence of 2,8-dihydroxyadenine crystals, and extracellular matrix collagen compared with CKD rats. In addition, the eGFR in the treatment group was similar to healthy rats, renal morphology was restored, and inflammatory cells were significantly lower. In conclusion, pioglitazone has a nephroprotective effect when administered in the early stages of kidney damage, reducing inflammatory and fibrotic processes and improving glomerular filtration rate. Furthermore, in the late phase of treatment, a tendency to decrease creatinine and increase eGFR was observed.

## Introduction

Chronic kidney disease (CKD) is defined by a decrease of glomerular filtration rate (eGFR) to <60 ml/min per 1.73 m<sup>2</sup>, which results in the loss of function due to kidney damage (1). In addition, it is a comorbidity that affects the world population with a prevalence of 13.4% (1990-2021) (2). For >30 years, the main causes of mortalities, morbidity and CKD risk factors worldwide, from birth to 95 years of age, have been studied. Mortality due to diabetes and CKD in 1990 ranked 14th and 18th, in 2019 ranked 8 and 9th and in 2021 ranked 10th and 11th, respectively (2,3). This shows that both CKD and diabetes have recently and considerably advanced as causes of mortalities in the world population, with the highest incidence in Latin America and the Caribbean. Diabetes and kidney diseases have a negative effect on life expectancy, resulting in a change in life expectancy that represents a global loss of 0.1 years in life expectancy (2).

---

*Correspondence to:* Dr Javier Ventura-Juárez, Department of Morphology, Center of Basic Sciences, Autonomous University of Aguascalientes, 940 University Avenue, 20100 Aguascalientes, Mexico  
E-mail: javier.ventura@edu.uaa.mx

Dr Sandra Luz Martínez-Hernández, Department of Microbiology, Center of Basic Sciences, Autonomous University of Aguascalientes, 940 University Avenue, 20100 Aguascalientes, Mexico  
E-mail: luz.martinez@edu.uaa.mx

**Key words:** chronic kidney disease, adenine, fibrosis, anti-inflammatory, pioglitazone

In Mexico, 11% of the population (~13 million individuals) have CKD (4,5). The main cause of CKD is type II diabetes mellitus, accounting for 12.8 million patients represent 30-50% of the CKD affected population (6). CKD is also triggered by arterial hypertension (27.2%), glomerulonephritis (8.2%), type 1 diabetes mellitus (3.9%), chronic tubulointerstitial nephritis (3.6%), cystitis (3.1%) of patients and, to a lesser extent, hereditary, autoimmune and obesity diseases (1,7). During the progression of the disease, an inflammatory response is generated, which triggers fibrosis, a tissue regeneration mechanism. It is accompanied by infiltration of cells of the immune response in renal tissue, synthesis and activation of pro-inflammatory cytokines and activation of fibroblasts and the consequent deposition of the extracellular matrix. Therefore, all these mechanisms facilitate the advancement of CKD, concluding with chronic renal failure (7).

Currently, drugs are used to treat patients with CKD, such as angiotensin-converting enzyme inhibitors to treat as a first-line antihypertensive therapy symptoms of hypertension in coronary diseases and cardiovascular conditions (8,9). However, in patients who cannot tolerate ACEI therapy due to an ACEI-induced cough or angioneurotic edema, angiotensin II receptor blockers (ARB) therapy is appropriate and suggested as an alternative to treat hypertension, congestive heart failure and diabetic nephropathy (8,10), angiotensin II (ATII) is the principal vasoactive peptide in the renin-angiotensin-aldosterone system and acts on two receptors, angiotensin 1 and 2 receptors (AT1 and AT2). ATII activation of AT1 receptors increase blood pressure due to contraction of vascular smooth muscle, increase systemic vascular resistance, increase sympathetic activity, sodium (Na), and water retention due to increase Na<sup>+</sup> reabsorption in the proximal convoluted tubule. Sodium reabsorption in the proximal convoluted tubule is a direct result of ATII and indirectly by increased aldosterone production in the adrenal cortex, promoting distal Na reabsorption (11). Chronically high levels of ATII cause smooth muscle and cardiac muscle cell growth and proliferation, endothelial dysfunction, platelet aggregation, enhanced inflammatory responses, and mediation of apoptosis. On the other hand, the effects of ATII binding to AT2 receptors result in vasodilatation due to increased production of nitrous oxide and bradykinin (8). Furthermore, activation of AT2 receptors leads to renal sodium excretion. Agonism at AT2 receptors have anti-proliferative and cardiovascular protective effects (10);  $\beta$  adrenergic receptor blockers in patients with hypertension and CKD (9,12); statins, which decrease cholesterol in patients with coronary diseases and in early stages of CKD block the formation of atherosclerosis and the onset of hypertension (9); xanthine oxidase inhibitors, which reduce levels of uric acid in serum (9); and antidiabetics [for example, sulfonylureas (depolarization of Ca<sup>2+</sup> channels in pancreatic  $\beta$  cells, secretagogue effect)] (13); dipeptidyl-peptidase 4 receptor inhibitors (resisting oxidation, inflammation, and fibrosis, destroying the advanced glycation end product (AGE)-RAGE signaling pathway and raising the levels of GLP-1, thereby improving endothelial dysfunction and providing multi-level kidney protection) (14); sodium-glucose cotransporter 2 inhibitor (reduces hyperglycemia in patients with type 2 diabetes by reducing the renal reabsorption of glucose, thereby increasing urinary glucose excretion) (15);  $\alpha$ -glucosidase inhibitor

(reversibly inhibits intestinal alpha-glucosidases, enzymes responsible for the metabolism of complex carbohydrates into absorbable monosaccharide units). This action results in a diminished and delayed rise in blood glucose following a meal (16); thiazolidinediones/glitazones (peroxisome proliferator activated receptors (PPARs) agonists) (affect nuclear receptors (PPAR) and subsequently enhance the effects of insulin) (17,18), which decrease serum glucose values.

Pioglitazone (5-[[4-[2-(5-ethylpyridin-2-yl)ethoxy]phenyl]methyl]-1,3-thiazolidine-2,4-dione;hydrochloride) (19) belongs to the family of thiazolidinediones/glitazones agonists of PPAR $\gamma$  and partial activators of PPAR $\alpha$ . It is widely used in the treatment of patients with type II diabetes because it regulates genes involved in adipogenesis, fatty acid oxidation and the increase in adiponectin secretion by adipocytes (16,17). Adiponectin activates muscle and hepatic AMPK, which stimulates fatty acid oxidation, which indirectly improves insulin sensitization related to obesity, increasing glucose uptake by cells through GLUT4 translocation (20-23). In recent decades PPARs have stood out as homeostatic modulators as they act as transcription factors, which coordinate various renal processes such as lipid and glucose metabolism, fatty acid oxidation and inflammatory responses. Some findings have shown that the deregulation of these receptors contributes to the progression of some diseases such as diabetes and cancer (24).

PPAR family consists of PPAR $\alpha$ , PPAR $\beta/\delta$  and PPAR $\gamma$ , which regulate fatty acid oxidation, adipogenesis, lipogenesis, glucose metabolism and insulin sensitivity (24). PPARs are widely distributed in the kidney, particularly, PPAR $\gamma$  is found in the distal collecting ducts and, in smaller amounts, they are also found in mesangial cells, podocytes and endothelial cells (25). Likewise, PPAR $\gamma$  coordinates various functions, such as adipocyte differentiation, lipid absorption and storage, thermogenesis, lipogenesis, oxidative stress, glucose absorption, and insulin signaling (24). PPAR $\gamma$  also participates in the negative regulation of NF- $\kappa$ B, as studies have highlighted the beneficial effect in the inflammatory and fibrotic process (26,27). Pioglitazone, which acts by stimulating PPAR $\gamma$  receptors, has been used in models of kidney damage; Ko *et al* (28) administered 10 mg/kg pioglitazone to diabetic nephropathy rats, showed the downregulation of genes involved in fibrosis and extracellular matrix deposition, such as TGF- $\beta$ 1, plasminogen activator inhibitor-1 and type IV collagen, through the decrease of NF- $\kappa$ B activity, MCP-1 and collagen synthesis. On the other hand, Németh *et al* (26) proposed that pioglitazone acts as a protective drug in renal fibrosis induced by TGF- $\beta$  by repressing the signaling pathways of EGR-1, STAT3 and AP-1 in a model with knockout mice that expressed increased levels of TGF- $\beta$ . Similarly, Sun *et al* (29) demonstrated that pioglitazone attenuates renal fibrosis by decreasing damage caused by ureteral obstruction through the decrease in the expression of fibronectin,  $\alpha$ -SMA and collagen I.

The aim of the present study was to analyze the anti-inflammatory and antifibrotic effects of pioglitazone in a rat model of CKD in an adenine-induced. Adenine is a purine base and high consumption or administration is immediately metabolized to 2,8-dihydroxyadenine (DHA) by xanthine oxidase (30,31). 2,8-DHA precipitates and forms crystals with low solubility resulting in recurrent urolithiasis leads

Table I. Primer sequences for reverse transcription-quantitative PCR.

Gene	Primer	Sequence (5'-3')	pb	Amplicon (pb)
Col-1	Fw	AGGCATAAAGGGTCATCGTG	20	157
	Rv	ACCGTTGAGTCCATCTTTGC	20	
ACTA-2	Fw	GCCAGTCGCCATCAGGAAC	19	74
	Rv	CACACCAGAGCTGTGCTGTCTT	22	
TGF- $\beta$	Fw	GACTCTCCACCTGCAAGACCA	21	244
	Rv	CGGGTGACTTCTTTGGCGTA	20	
$\beta$ -actin	Fw	GTCGTACCACTGGCATTGTG	20	175
	Rv	GCTGTGGTGAAGCTGTA	20	

Col-1, Collagen type 1; ACTA-2,  $\alpha$ -SMA; Fw, forward; Rv, reverse.

to secondary nephropathy (32). The adenine model has been widely used to generate kidney damage because its metabolic alterations reproduce CKD characterized by crystalline deposits, foreign body granulomas formation in the renal tubules and interstitium, and increase fibrosis and inflammation, leading to tubule-interstitial disease; these abnormalities are similar to the symptoms of CKD in humans (32). Most animal models do not mimic the complexity of the human disease; however, the adenine model of CKD in rodents is an exception (33).

## Materials and methods

**Animals and ethical approval.** A total of 40 male Wistar rats between 150-250 g (age, 6 weeks old), were obtained from the animal facility at the Basic Sciences Center of the Autonomous University of Aguascalientes (Aguascalientes, Mexico). The animals were kept in light/dark cycles of 12 h, relative humidity and controlled temperature of 25°C. They were previously dewormed (fenbendazole 55 mg, toltrazuril 20 mg and praziquantel 10 mg) at a dose of 1 ml/kg, intragastric, for 3 days. Likewise, throughout the experimentation, a diet based on Purina Rodent Chow Nutricubes (cat. no H87 Nestlé, Purina, Mexico) and purified water were provided with free access. All animal experiments were approved by the Ethics Committee for the use of animals in teaching and research at UAA (CEADI-UAA, UAA: Autonomous University of Aguascalientes, AUT-B-C-1121-077-Tipo C; approval no. CEADI-02-2023), following the Mexican Official Standard NOM-062-ZOO-1999 (34), and the guidelines of the National Institutes of Health for the care and use of Laboratory animals (35). During the experiment, various signs related to humane endpoints were monitored weekly, including stress, pain, decreased mobility, withdrawal, weight loss, reduced food and water intake, self-mutilation and behavioral changes such as aggressiveness.

**Experimental design.** To evaluate the effects of pioglitazone in early and late stages of CKD, two experimental groups were used.

*i) The therapeutic group.* The rats were divided into three sub-groups (n=5): a) intact (healthy); b) adenine (CKD); and c) adenine/pioglitazone (treatment). The induction of

CKD was performed by administering 150 mg/kg/day of adenine (cat. no. A8626; Sigma-Aldrich; Merck KGaA) for 4 weeks, the route of administration was oral and for this, a curved stainless steel esophageal cannula (18x3"; Cadence Science) was used. Once the induction was finished, the treatment was started, which consisted of the administration of 60 mg/kg/day pioglitazone (Pharmalife LTC) (36-38) diluted in 0.5% carboxymethylcellulose for 5 weeks.

*ii) The prophylactic group.* The rats were divided into five sub-groups (n=5): a) intact (healthy); b) adenine (CKD); c) endogenous reversion (recovery without treatment); d) adenine/pioglitazone (treatment); and e) pioglitazone. For the prophylactic group, the induction of kidney damage (CKD) and the administration of the treatment (pioglitazone) was performed simultaneously, the induction time of CKD was 4 weeks, and the treatment time was 7 weeks (Fig. 1).

At the end of the treatments, all rats were euthanized with an overdose of sodium pentobarbital ( $\geq 100$  mg/kg) intraperitoneally, until rapid loss of consciousness, thus minimizing stress and anxiety experienced by the animal, monitoring respiratory and cardiac signs until their absence. During euthanasia, renal tissue and blood samples were immediately collected and processed, additionally, biomarkers of renal damage and gene expression were analyzed. It is worth mentioning that the group that was only administered pioglitazone was to evaluate the toxicity of the drug. Euthanasia was carried out following accepted animal euthanasia methods based on the guidelines of the American Veterinary Medical Association (AVMA) (39). The blood collection was carried out as a non-survival procedure.

**Biomarkers of renal damage.** By colorimetry in in the Dimension EXL-200 (Siemens AG), the blood concentration of the metabolites urea, creatinine and uric acid were determined. From the measurement of urea and creatinine, the eGFR was calculated using the formula proposed by Besseling *et al* (40).

**Histopathological study.** Hematoxylin-eosin (H&E) staining was performed for evaluation of tissue damage and Masson's trichrome and Sirius Red staining were performed for visualization of extracellular matrix and collagen fibers. The kidneys were processed with automatic tissue processors (Microm STP 120, Thermo Fisher Scientific). Tissue sections were obtained

at 5  $\mu\text{m}$  thickness, using a rotation microtome (Leica RM, 2125RT). The staining process started with deparaffinization in a 60°C laboratory oven for 1 h. The tissues were placed in two xylol (100%), and alcohol (100 and 96%) solutions and transferred to distilled water. For hematoxylin and eosin staining, rehydrated slides were immersed in hematoxylin solution (cat. no HX9125853 Merck KGaA) at room temperature for 3 min, then rinsed briefly in tap water. Slides were then dipped in acid alcohol for a few sec to remove excess hematoxylin and rinsed with tap water. Counterstaining with eosin started with immersing in eosin Y working solution (cat. no HX20198139 Merck KGaA) at room temperature for 2.5 min and rinsing with tap water. Sirius Red staining, the rehydrated slides were immersed in Weigert's hematoxylin for 8 min and washed with tap water and PBS-1X. The slides were placed at room temperature for 1 h in Picro-Sirius Red Stain (0.5% Sirius red cat. no 2610-10-8 Sigma-Aldrich; Merck KGaA), and excess dye was removed. Masson's trichrome staining, the rehydrated slides were immersed at room temperature overnight in Bouin's fixative solution (formalin 10%). The slides were rinsed briefly in tap water and distilled water. Subsequently, the slides were incubated at room temperature; in Weigert's hematoxylin for 10 min (Sol. A 1% hematoxylin in 96% alcohol, Sol. B: 1.16 g iron chloride + 1 ml 25% of hydrochloric acid in 99 ml distilled water. In relation 1:1, sol A/sol B), Biebrich solution (1% Biebrich scarlet in 1% acid fuchsin and 1 ml acetic acid) for 15 min, phosphomolybdic 5% and phosphotungstic 5% in distilled water for 15 min and counterstain in aniline blue solution (5% blue aniline, 2 ml acetic acid glacial, 100 ml distilled water) for 10 min. The slides were rinsed with 1% acetic acid in distilled water.

Finally, all the slides were performed by transferring through a series of ethanol solutions (96 and 100%). The slides were cleared in xylene and covered by Tissue-Tek (cat. no HX90832861, Merck KGaA). Image analysis was performed through the Axioscope 40/40 FL fluorescence microscope (Zeiss AG) and processed with the Image ProPlus Software 4.5.1 (Media Cybernetics).

**Molecular biomarkers.** Reverse transcription-quantitative PCR (RT-qPCR). Total RNA extraction was performed using the Direct-zol™ RNA MiniPrep kit (cat. no. R2050; Zymo Research Corp.) following the manufacturer's specifications. The RNA was quantified using the Biodrop (cat. no. 80-3006-51; Isogen Life Science B.V.) equipment and subsequently the RNA was stored at -80°C. For the cDNA obtainment, reverse transcription was performed with 1  $\mu\text{g}$  of RNA using GoScript™ Reverse Transcription System (cat. no. A5000; Promega Corp.). Subsequently, qPCR was performed using the Maxima SYBR Green/ROX qPCR Master Mix (2X) (cat. no. K0221; Thermo Fisher Scientific, Inc.), using StepOne™ Real-Time PCR Systems (Applied Biosystems) to evaluate the relative expression of the genes: Collagen 1,  $\alpha$ -SMA and TGF- $\beta$ . Thermocycling conditions were as follows: 95°C for 3 min for initial denaturation, 40 cycles of 95°C for 30 sec of denaturation, and 62°C for 45 sec for annealing. The oligonucleotide primers are shown in Table I. The relative expression levels were normalized with respect to those of  $\beta$ -actin, and the differences were determined by the  $2^{-\Delta\Delta C_q}$  method (41).

**Statistical analysis.** Statistical analysis was performed using GraphPad Prism 8.0.2 software (Dotmatics). Differences mean  $\pm$  standard error of the mean between groups were assessed using non-parametric multi-group analysis of variance with Kruskal-Wallis test with a post hoc Dunn's test for multiple groups or Mann-Whitney U test for two groups  $P < 0.05$  was considered to indicate a statistically significant difference,  $n=3$ .

## Results

**Pioglitazone restores renal function but does not promote regeneration of tubular architecture in a therapeutic group.** A macroscopic indicator of renal damage process is the measurement of the kidney index. This index is calculated by assessing the total weight of the animal with the weight of both kidneys. Its purpose is to assess whether there are changes in renal mass. Our results indicate that the kidney index in the therapeutic group does not show significant differences with respect to the intact, adenine and adenine/pioglitazone sub-groups (Fig. 2A). On the other hand, the kidney function tests evaluated by the serum measurement of creatinine, urea, eGFR and uric acid (Fig. 2B-E), showed that creatinine is lower in the adenine/pioglitazone sub-group (0.57 mg/dl) compared with the adenine sub-group (1.05 mg/dl;  $P=0.414$ ), and creatinine in adenine/pioglitazone sub-group is similar to the intact sub-group (0.40 mg/dl;  $P=0.939$ ) (Fig. 2B). By contrast, the amount of urea in the adenine/pioglitazone sub-group (123.75 mg/dl) was similar to the adenine sub-group (127.38 mg/dl;  $P>0.999$ ) and to intact sub-group (59.52 mg/dl) without significant difference (Fig. 2C). The eGFR was higher (1.06 ml/min) in relation to the adenine (0.45 ml/min;  $P=0.539$ ), indicating a possible restoration of renal function. Moreover, a decrease in serum uric acid levels was found in the adenine sub-group (1.58 mg/dl) compared with the intact sub-group (2.41 mg/dl;  $P=0.529$ ), while the levels in the adenine/pioglitazone sub-group (3.61 mg/dl;  $P>0.999$ ) were similar to the intact sub-group (Fig. 2E).

The histopathological analysis showed that pioglitazone does not attenuate the inflammatory response, did not decrease levels of cellular infiltration as abundant inflammatory cells are observed in some glomeruli and the intertubular space of the renal corticomedullary zone similar to what is observed in the adenine sub-group (Fig. 2F and G). The morphometric analysis of Masson's staining shows a higher percentage of collagen fibers in adenine-treated animals was markedly lower in pioglitazone-treated animals (Fig. 2H). The analysis of transcription levels of genes related to inflammation and fibrosis, collagen type 1,  $\alpha$ -SMA and TGF- $\beta$  (Fig. 2I-K) did not show significant differences between the sub-groups. However, TGF- $\beta$  showed a lower level of expression in adenine/pioglitazone sub-group compared with untreated animals.

**Pioglitazone improves renal function and attenuates the progression of damage in the prophylactic group.** The macroscopic analysis of the effect of pioglitazone on the kidney is depicted in Fig. 3. The upper part of Fig. 3A shows kidney damage induced by adenine in rats, with abundant deposits of 2,8-DHA crystals in the cortico-medullary zone of the kidney. Conversely, the lower part of Fig. 3A corresponds to a kidney induced with adenine

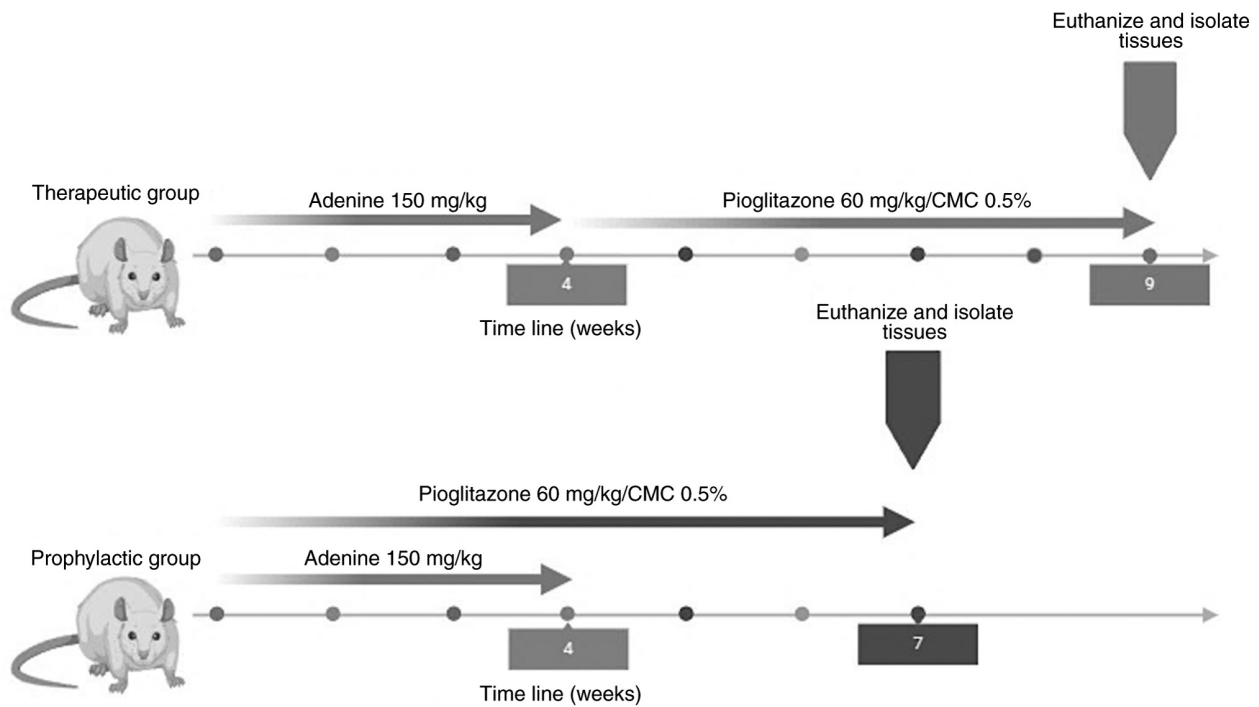


Figure 1. Experimental design, considering adenine application times and pioglitazone treatments. CMC, carboxymethyl cellulose.

and treated with pioglitazone, demonstrating the absence of abundant 2,8-DHA crystals. In the lower inset, the presence of a crystal in the process of degradation in the renal parenchyma is highlighted. On the other hand, the quantification of 2,8-DHA crystals in rats treated with adenine and adenine/pioglitazone showed a higher number of crystals in untreated rats compared to those treated (Fig. 3B). The rats treated with pioglitazone had a lower kidney index, which was similar to the intact sub-group (Fig. 3C). Likewise, pioglitazone restores renal function, lowering serum creatinine (0.704 mg/dl;  $P=0.895$ ) and urea (66.34 mg/dl;  $P=0.023$ ), and concomitantly increases the eGFR (1.38 ml/min;  $P=0.0315$ ) that is mostly significant in relation to the adenine (0.452 ml/min) and endogenous reversion (1.14 ml/min;  $P=0.2575$ ). This reduction was also found in the measurement of uric acid (2.06 mg/dl;  $P=0.044$ ), where it is significant in relation to the adenine (3.47 mg/dl) (Fig. 3D-G). On the other hand, the histopathological analysis demonstrated that pioglitazone attenuated the inflammatory response and the cellular infiltration by decreasing the number of inflammatory cells and deposition of the extracellular matrix and collagen fibers, since the renal morphology in adenine/pioglitazone sub-group is like that of the intact sub-group (Fig. 3H). Notably, inflammatory cells were counted per interstitial area of kidneys treated with adenine and pioglitazone (Fig. 3I). Masson's morphometric staining analysis showed a higher percentage of collagen fibers in the adenine-treated animals while the percentage in the pioglitazone-treated animals was significantly lower (Fig. 3J). This finding is also reflected in the decrease of the expression of collagen type 1,  $\alpha$ -SMA and TGF- $\beta$  (Fig. 3K-M). These effects of pioglitazone were attributed to the drug administered and not the recovery of the organism itself (endogenous reversion group), since the results obtained in the endogenous reversion only reflect the capacity of restoration of renal function, but not of the regeneration of renal morphology (Fig. 3).

*Pioglitazone does not show toxicity in healthy kidneys at 7 weeks in a Wistar rat model.* The renal function tests, the histopathological and molecular analysis demonstrated that the administration of 60 mg/kg of pioglitazone to healthy Wistar rats for 7 weeks did not generate toxicity, since no significant differences were observed in relation to the intact (Fig. 4).

## Discussion

In tubulointerstitial injury, the cells commonly involved are tubular epithelial cells, fibroblasts, fibrocytes, myofibroblasts, monocytes, macrophages and mast cells. In addition, molecular markers such as TGF- $\beta$ , BMP, PDGF and HGF are involved (42). Particularly, the increase of TGF- $\beta$  signaling correlates with the onset and progression of fibrosis, as it promotes the activation of fibroblasts, synthesis and expression of extracellular matrix proteins, such as collagen (43). The mechanisms of tissue repair and restoration in the presence of kidney damage trigger the accumulation of dysfunctional connective tissue. The inflammatory process and the increase of extracellular matrix impair the renal parenchyma being a triggering mechanism of renal failure (44,45).

Some easy-to-use substances, such as neutral electrolyzed saline, have been used to alleviate the renal inflammatory/fibrotic process (46). Due to the high worldwide prevalence of CKD and the poor effectiveness of current drugs in the progression of the disease, it is for this reason that, in the present study, the effects of pioglitazone as a potential treatment of CKD were evaluated by repressing the inflammatory and fibrotic processes triggered in two experimental groups of adenine-induced renal damage (therapeutic and prophylactic groups). This was to demonstrate the beneficial effects of the drug on the damage caused by adenine. Studying two types of simultaneous comparative experimental groups allowed the present study to identify the

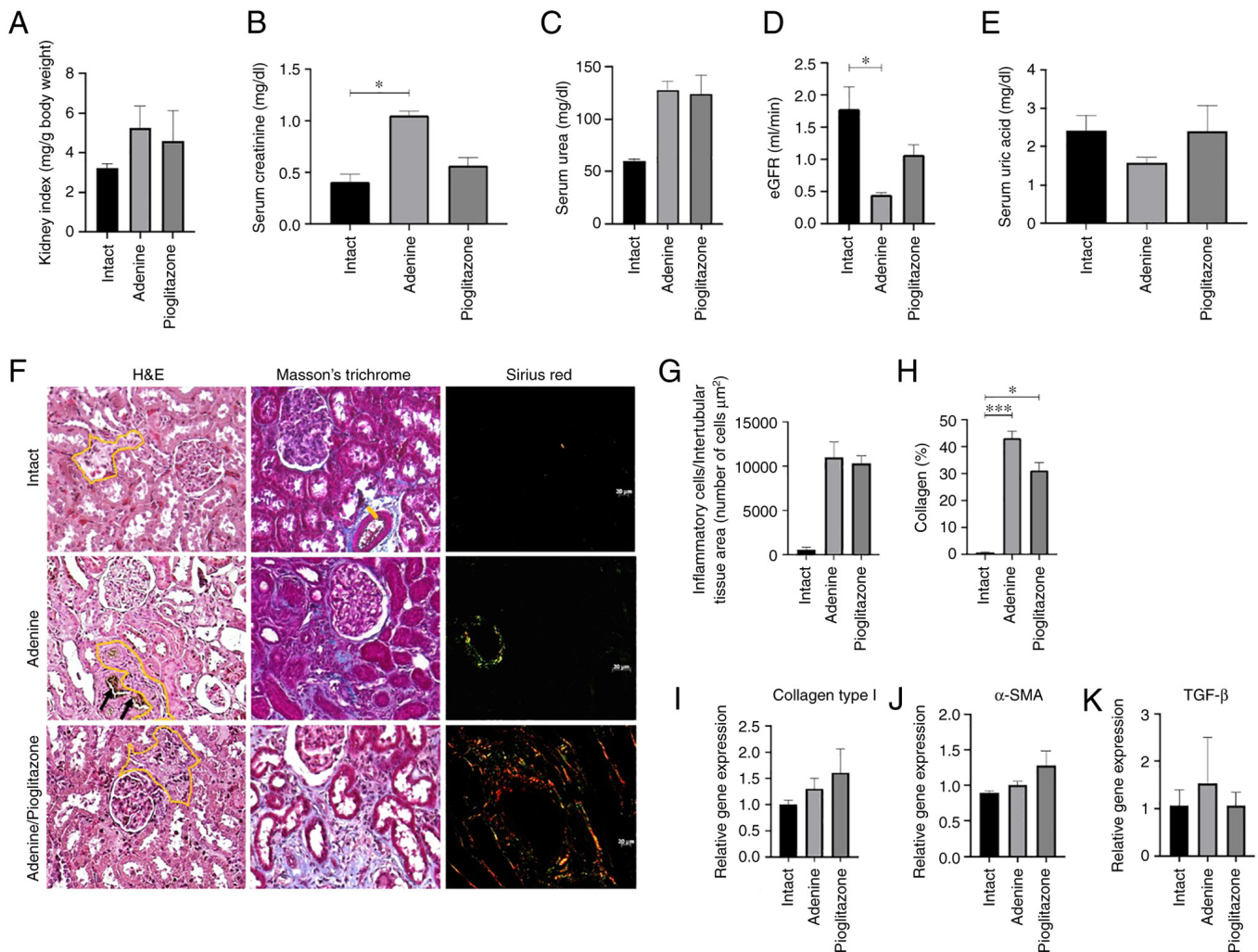


Figure 2. Pioglitazone restores renal function by partially increasing eGFR and decreasing type 1 collagen deposition in the therapeutic group. (A) Kidney index, with no significant differences between the groups. (B-E) Biomarkers of renal damage, measuring (B) creatinine, (C) blood urea, (D) eGFR and (E) blood uric acid; eGFR was determined from the measurement of creatinine and blood urea nitrogen. (F) Histopathological analysis of renal tissues fixed in neutral formalin, stained with hematoxylin/eosin, Masson's trichrome and Sirius red. Black arrows indicate the deposition of 2,8-DHA crystals. Yellow line shows the interstitial zone with inflammatory infiltrate. Magnification, x200. (G) Quantification of inflammatory infiltrate cells in renal interstitial zone. (H) Morphometric analysis of the amount of collagen deposited in renal interstitial tissue by Masson's trichrome stain. Expression of genes (I) collagen type 1, (J)  $\alpha$ -SMA, and (K) TGF- $\beta$ . \* $P < 0.05$ ; \*\*\* $P < 0.001$ . eGFR, glomerular filtration rate.

pathophysiological mechanisms that lead to inflammation and subsequent renal fibrosis (45) and enabled the proposal of new drugs that counteract the damage in early and late stage of CKD.

The results obtained from the therapeutic group of the present study showed that pioglitazone did not manage to reverse the damage in the renal tissue through the attenuation of the inflammatory process and cellular infiltration, since, according to the histopathological analysis in the Masson's trichrome and Sirius red staining, the presence of extracellular matrix and collagen fibers, predominantly type 1 and, were observed. Likewise, the molecular analysis showed an increase in the expression of collagen type 1,  $\alpha$ -SMA and TGF- $\beta$  of the rats treated with pioglitazone. However, the renal function tests show a marked improvement in the eGFR and creatinine. The eGFR is widely accepted and used as a parameter that reflects renal function in general (47) and can be calculated from the concentrations of creatinine and urea. Likewise, creatinine is a freely filtered molecule, so it is used as a marker of renal function (48). Similar to creatinine, blood

urea is controlled by the eGFR since the concentration of this in the ultrafiltrate is similar to that of plasma (49). The eGFR in the adenine sub-group was low compared with the intact sub-group, indicating that renal function decreased because of the induced damage. These findings were also described by the authors Zhu *et al* (47), where they highlight the 57% renal decrease after the administration of adenine in rats. Consistent with this, the creatinine values were lower in the adenine/pioglitazone sub-group with respect to the adenine sub-group. Likewise, the sub-group treated with pioglitazone presented with uremia at 5 weeks. As mentioned by Singh *et al* (45), tubulointerstitial fibrosis strongly correlates with renal function and represents a complex change in the architecture of the kidney, which includes the activation of proteases, production of MMP, collagen by epithelial cells and activated myofibroblasts. However, the results obtained in the present study show that, despite the interstitial fibrosis generated by adenine, pioglitazone restores renal function at 7 weeks by increasing the eGFR.

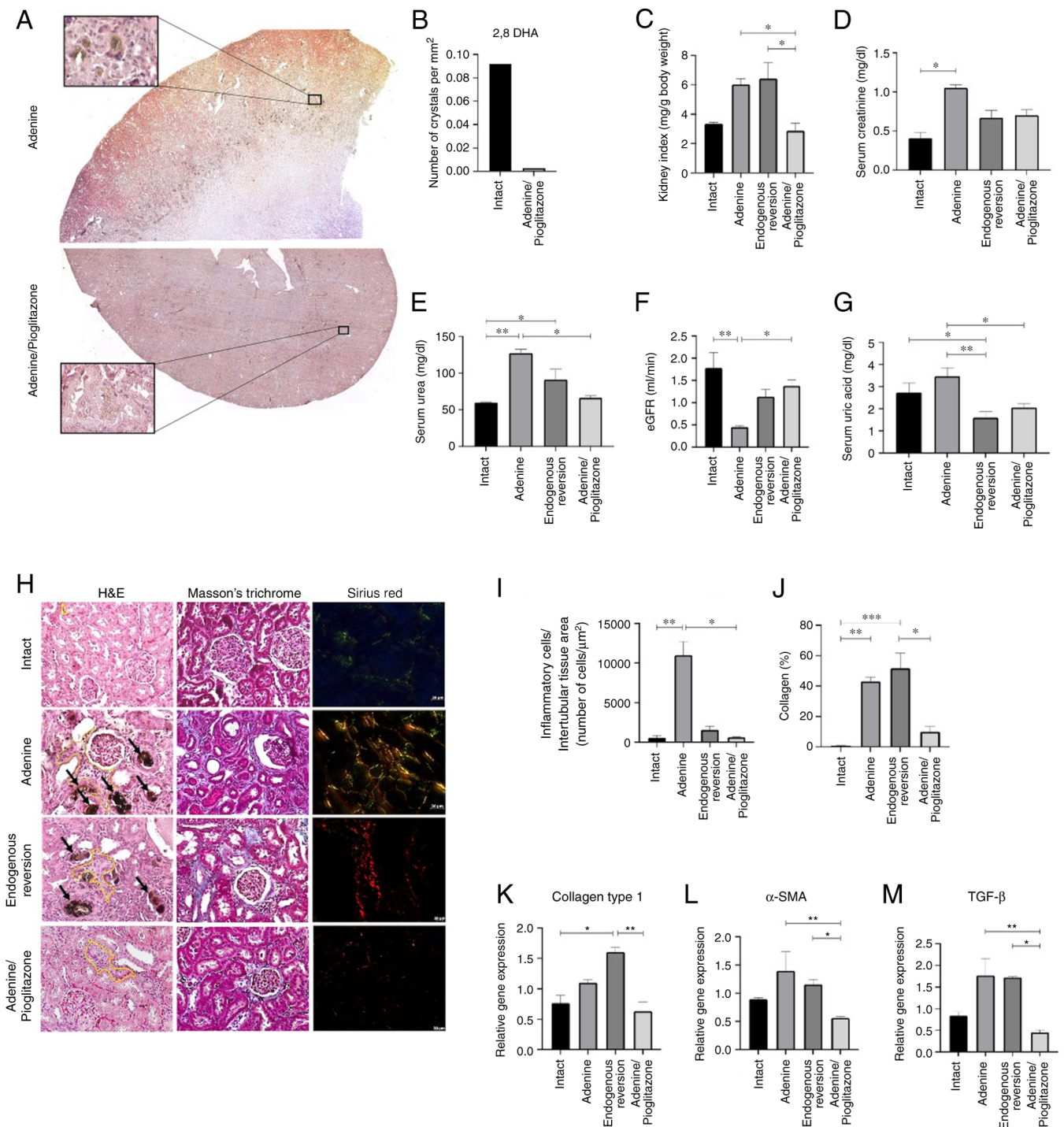


Figure 3. Pioglitazone reduces 2,8-DHA crystals, restores renal function, and decreases inflammation and fibrosis in the prophylactic group. (A) Panoramic images of kidneys treated with adenine and adenine/pioglitazone increased accumulation of 2,8-DHA crystals is observed in the corticomedullary zone in the adenine group. Magnification, X5, X400. (B) Quantification of 2,8-DHA crystals. (C) Kidney index. Biomarkers of renal damage, measuring (D) creatinine, (E) blood urea nitrogen, (F) eGFR and (G) uric acid; eGFR was determined from the measurement of creatinine and blood urea nitrogen. (H) Histopathological analysis of renal tissues fixed in neutral formalin, stained with hematoxylin/eosin, Masson's trichrome and Sirius red. Black arrows indicate the deposition of 2,8-DHA crystals. Yellow line indicates the interstitial zone with inflammatory infiltrate. Magnification, x200. (I) Quantification of inflammatory infiltrate cells in renal interstitial zone. (J) Morphometric analysis of the amount of collagen deposited in renal interstitial tissue by Masson's trichrome stain. Expression of genes (K) collagen type 1, (L)  $\alpha$ -SMA and (M) TGF- $\beta$ . \*P<0.05; \*\*P<0.01; \*\*\*P<0.001. eGFR, glomerular filtration rate.

Consistent with this, the vasculoprotective properties of pioglitazone have also been demonstrated in a previous study, as it increases the expression of endothelial nitric oxide synthase and neuronal nitric oxide synthase that regulates glomerular blood flow and eGFR through the regulation of

vascular tone in the afferent arterioles (50). Unlike the therapeutic group, in the present study, the results of the prophylactic group demonstrated that pioglitazone at 7 weeks restored renal function and attenuated inflammation, as the results of the biochemical analysis showed a high value of eGFR compared

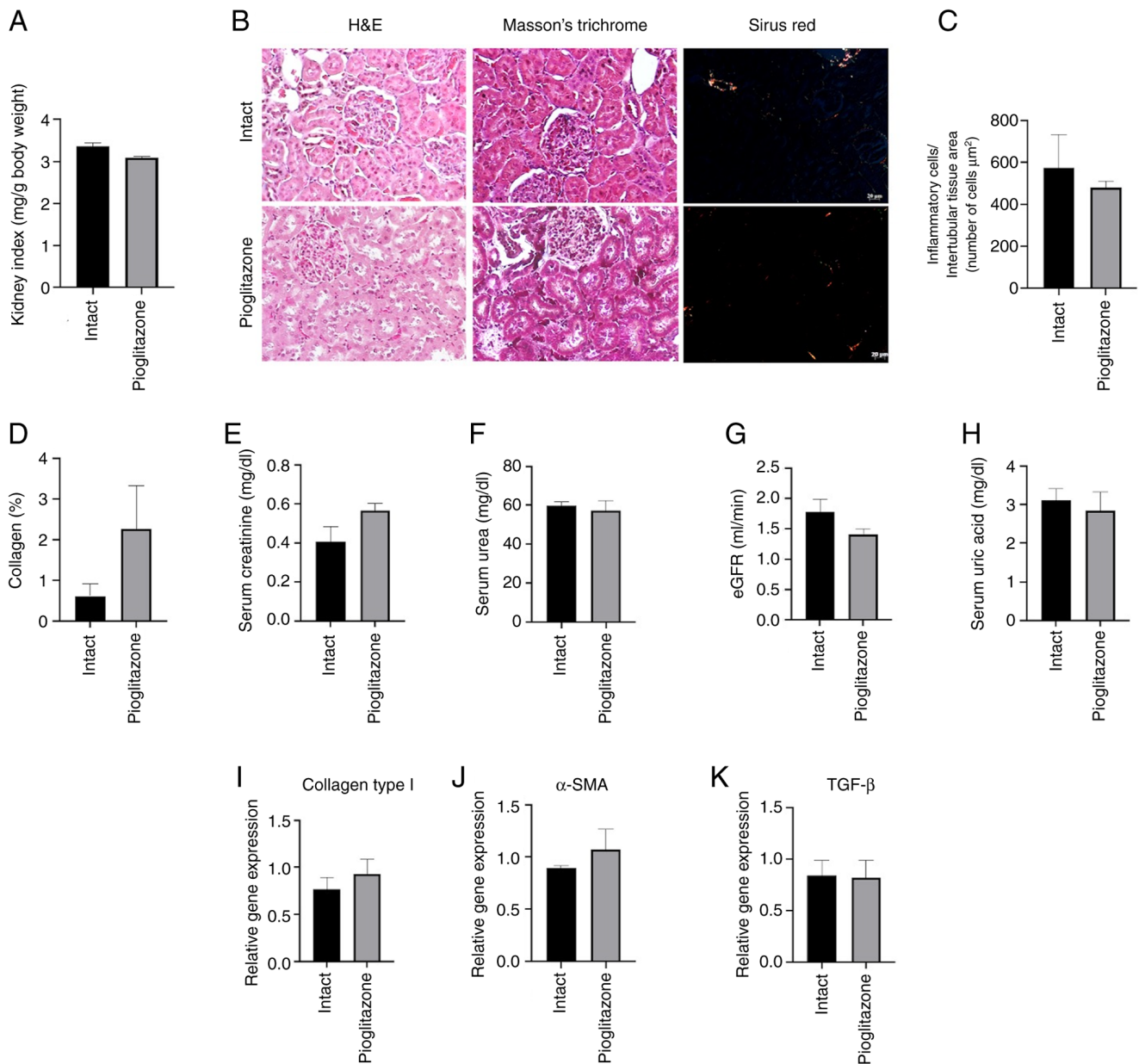


Figure 4. Administration of pioglitazone does not show toxicity in healthy kidneys at 7 weeks in a Wistar rat model. (A) Kidney index (no significant differences). (B) Histopathological analysis of renal tissues fixed in neutral formalin, stained with hematoxylin/eosin, Masson's trichrome and Sirius red. Magnification, x200). (C) Quantification of inflammatory infiltrate cells in renal interstitial zone. (D) Morphometric analysis of the amount of collagen deposited in renal interstitial tissue by Masson's trichrome stain. Biomarkers of renal damage, measuring (E) creatinine, (F) blood urea nitrogen, (G) eGFR and (H) uric acid; eGFR was determined from the measurement of creatinine and blood urea nitrogen. Expression of genes (I) collagen type 1, (J)  $\alpha$ -SMA and (K) TGF- $\beta$ . eGFR, glomerular filtration rate.

with the adenine and endogenous reversion animals. In adenine/pioglitazone sub-group the histopathological analysis, a lower deposit of 2,8-DHA crystals was observed during H&E staining, and a lower amount of type 1 and 3 collagen fibers were revealed using Sirius red staining compared with the adenine and endogenous reversion. Likewise, the panoramic images demonstrated the reduction of crystals in the cortico-medullary zone of the group treated with pioglitazone compared to the group treated with adenine.

According to Asplin *et al* (51) and Maalouf *et al* (52), by sensitizing insulin, pioglitazone increases the pH of the urine and thus avoids the formation of uric acid stones. The present study corroborated this with the results obtained in

the measurement of serum uric acid, where low values were observed in the rats treated with pioglitazone compared with the adenine and endogenous reversion groups. Similarly, the molecular analysis corroborated that pioglitazone lowered the extracellular matrix deposits and amount of collagen fibers compared with adenine and endogenous reversion sub-groups, as it showed the decrease of the expression of collagen type 1,  $\alpha$ -SMA and TGF- $\beta$ .

This can be attributed to an inhibition of TGF- $\beta$  through two pathways: i) The signaling of TGF- $\beta$  acts through the SMAD pathway. The positive regulation of SMAD7 can suppress the signaling of TGF- $\beta$ -SMAD by activating the p65 subunit of NF- $\kappa$ B (53). Studies have shown that PPAR $\gamma$



agonists decrease the expression of TGF- $\beta$ 1 and the phosphorylation of SMAD2/3 while increasing the expression of SMAD7 (54), as well as protein Lefty-1 (55). ii) The direct inhibition of NF- $\kappa$ B through the PPAR $\gamma$  agonist. PPAR $\gamma$  act as an E3 ubiquitin ligase that interacts with the p65 subunit of NF- $\kappa$ B to induce its ubiquitination and subsequent degradation, which attenuates the inflammation caused by the NF- $\kappa$ B pathway (56). Pioglitazone, by inhibiting the inflammatory pathway of NF- $\kappa$ B, attenuates the fibrotic process (epithelial-mesenchymal transition and collagen deposit) (57). Also, the antioxidant properties of pioglitazone have been revealed to increase the expression of SOD levels and decrease the levels of MDA, which contributes to the restoration of the antioxidant capacity (58) and cell regeneration.

Therefore, the results of the present suggested that the administration of pioglitazone for 7 weeks in early stages could slow down or prevent the progression of CKD, possibly due to a pathway of cell regeneration that is increased by the metabolism of lipids and carbohydrates (59). This, in addition to improving the absorption of lipids and carbohydrates through different pathways and mediating the oxidative stress as aforementioned, under negative feedback of the inflammatory pathway of NF- $\kappa$ B, could attenuate and/or reverse the progression of interstitial fibrosis induced by adenine, as well as restore the function of the renal parenchyma given by an increase in eGFR.

In conclusion, in early stages of CKD, pioglitazone, by stimulating the PPAR $\gamma$  pathway, counteracts the profibrotic and inflammatory mechanisms triggered during the disease, improving function and promoting the regeneration of renal morphology by reducing the expression of TGF- $\beta$ ,  $\alpha$ -SMA and type 1 collagen. However, in the late phase of treatment, pioglitazone improved renal function by increasing eGFR and slightly decreasing serum creatinine.

### Acknowledgements

Not applicable.

### Funding

This research was funded by Autonomous University of Aguascalientes (grant nos. PIBB22-10N, PIBB23-6) and National Council for the Humanities, Science and Technology (grant no. 32029).

### Availability of data of materials

The data generated in the present study may be requested from the corresponding author.

### Authors' contributions

MPV, JVJ and SMH designed the article structure and revised the manuscript. JMG, ABG and NGC made substantial contributions to conception and design and wrote the manuscript. JMG performed the literature review. MMO and ESA contributed to the acquisition, analysis and interpretation of the data and prepared the figures. MAB analyzed data. SMH and MAB confirm the authenticity of all the raw data. All authors have read and confirmed the final version of the manuscript.

### Ethic approval and consent to participate

All the experiments of this study were governed by the NOM-062-ZOO-1999 (34) (Mexican standard) and were approved (approval no. CEADI-UAA-02-2023) by the Institutional Bioethics Committee for the Management of Laboratory Animals, which is based on the guidelines of the National Institutes of Health for the care and use of Laboratory animals (NIH publications no. 8023).

### Patient consent for publication

Not applicable.

### Competing of interests

The authors declare that they have no competing interests.

### References

- Vaidya SR and Aeddula NR: Chronic Kidney Disease. In: StatPearls. StatPearls Publishing, Treasure Island (FL), 2023.
- Naghavi M, Ong KL, Aali A, Ababneh HS, Abate YH, Abbafati C, Abbasgholizadeh R, Abbasian M, Abbasi-Kangevari M, Abbastabar H, *et al*: Global burden of 288 causes of death and life expectancy decomposition in 204 countries and territories and 811 subnational locations, 1990-2021: A systematic analysis for the Global Burden of Disease Study 2021. *Lancet* 403: 2100-2132, 2024.
- Murray CJL: The global burden of disease study at 30 years. *Nat Med* 28: 2019-2026, 2022.
- Colegio de Nefrólogos de México: Revista nefrología Mexicana-colegio de nefrólogos de México. *Nefrol Mex* 41: 34, 2020.
- Liu BC, Lan HY and Lv LL: Renal fibrosis: Mechanisms and therapies. Springer, Singapore, 2019.
- Arreola-Guerra JM, Gutiérrez-Peña CM, Zúñiga L, Ovalle-Robles I, García-Díaz AL, Macías-Guzmán MJ, Delgado A, Macías D, Prado C, Vega A, *et al*: Enfermedad renal Crónica en aguas calientes. ISEA México, 2019.
- Awad AM, Saleh MA, Abu-Elsaad NM and Ibrahim TM: Erlotinib can halt adenine induced nephrotoxicity in mice through modulating ERK1/2, STAT3, p53 and apoptotic pathways. *Sci Rep* 10: 11524, 2020.
- Herman LL, Padala SA, Ahmed I and Bashir K: Angiotensin-Converting Enzyme Inhibitors (ACEI). In: StatPearls. StatPearls Publishing, Treasure Island (FL), 2024.
- John M and Eisenberg Center for Clinical Decisions and Communications Science: Medicamentos para la enfermedad renal crónica en fase inicial. In: Las Guías Sumarias de los Consumidores. Agency for Healthcare Research and Quality (US), Rockville (MD), 2012.
- Hill RD and Vaidya PN: Angiotensin II Receptor Blockers (ARB). In: StatPearls. StatPearls Publishing, Treasure Island (FL), 2024.
- Crowley SD, Zhang J, Herrera M, Griffiths R, Ruiz P and Coffman TM: Role of AT1 receptor-mediated salt retention in angiotensin II-dependent hypertension. *Am J Physiol Renal Physiol* 301: F1124-F1130, 2011.
- Brunton L, Knollmann B and Hilal-Dandan R: Goodman and Gilman's the Pharmacological Basis of Therapeutics, 13th Edition. New York, 2017.
- Niemi M, Kivistö KT, Backman JT and Neuvonen PJ: Effect of rifampicin on the pharmacokinetics and pharmacodynamics of glimepiride. *Br J Clin Pharmacol* 50: 591-595, 2000.
- Liu J, Zhang J, Hou MH and Du WX: Clinical efficacy of linagliptin combined with irbesartan in patients with diabetic nephropathy. *Pak J Med Sci* 38: 52-56, 2022.
- Wanner C, Inzucchi SE, Lachin JM, Fitchett D, von Eynatten M, Mattheus M, Johansen OE, Woerle HJ, Broedl UC and Zinman B; EMPA-REG OUTCOME Investigators: Empagliflozin and progression of kidney disease in type 2 diabetes. *N Engl J Med* 375: 323-334, 2016.

16. Martin AE and Montgomery PA: Acarbose: An alpha-glucosidase inhibitor. *Am J Health Syst Pharm* 53: 2277-2290, 1996.
17. Lehmann JM, Moore LB, Smith-Oliver TA, Wilkison WO, Willson TM and Klier SA: An antidiabetic thiazolidinedione is a high affinity ligand for peroxisome proliferator-activated receptor gamma (PPAR gamma). *J Biol Chem* 270: 12953-12956, 1995.
18. Yamanouchi T: Concomitant therapy with pioglitazone and insulin for the treatment of type 2 diabetes. *Vasc Health Risk Manag* 6: 189-197, 2010.
19. PubChem CID 60560 for Chemical Safety: Pioglitazone Hydrochloride., 2024.
20. Ceddia RB, Somwar R, Maida A, Fang X, Bikopoulos G and Sweeney G: Globular adiponectin increases GLUT4 translocation and glucose uptake but reduces glycogen synthesis in rat skeletal muscle cells. *Diabetologia* 48: 132-139, 2005.
21. Ho CC, Yang YS, Huang CN, Lo SC, Wang YH and Kornelius E: The efficacy of pioglitazone for renal protection in diabetic kidney disease. *PLoS One* 17: e0264129, 2022.
22. Kubota N, Terauchi Y, Kubota T, Kumagai H, Itoh S, Satoh H, Yanai W, Ogata H, Tokuyama K, Takamoto I, *et al*: Pioglitazone ameliorates insulin resistance and diabetes by both adiponectin-dependent and -independent pathways. *J Biol Chem* 281: 8748-8755, 2006.
23. Yau H, Rivera K, Lomonaco R and Cusi K: The future of thiazolidinedione therapy in the management of type 2 diabetes mellitus. *Curr Diab Rep* 13: 329-341, 2013.
24. Libby AE, Jones B, Lopez-Santiago I, Rowland E and Levi M: Nuclear receptors in the kidney during health and disease. *Mol Aspects Med* 78: 100935, 2021.
25. Platt C and Coward RJ: Peroxisome proliferator activating receptor- $\gamma$  and the podocyte. *Nephrol Dial Transplant* 32: 423-433, 2017.
26. Németh A, Mózes MM, Calvier L, Hansmann G and Kökény G: The PPAR $\gamma$  agonist pioglitazone prevents TGF- $\beta$  induced renal fibrosis by repressing EGR-1 and STAT3. *BMC Nephrol* 20: 245, 2019.
27. Kaplan J, Nowell M, Chima R and Zingarelli B: Pioglitazone reduces inflammation through inhibition of NF- $\kappa$ B in polymicrobial sepsis. *Innate Immun* 20: 519-528, 2014.
28. Ko GJ, Kang YS, Han SY, Lee MH, Song HK, Han KH, Kim HK, Han JY and Cha DR: Pioglitazone attenuates diabetic nephropathy through an anti-inflammatory mechanism in type 2 diabetic rats. *Nephrol Dial Transplant* 23: 2750-2760, 2008.
29. Sun L, Xu T, Chen Y, Qu W, Sun D, Song X, Yuan Q and Yao L: Pioglitazone attenuates kidney fibrosis via miR-21-5p modulation. *Life Sci* 232: 116609, 2019.
30. Wyngaarden JB and Dunn JT: 8-Hydroxyadenine as the intermediate in the oxidation of adenine to 2,8-dihydroxyadenine by xanthine oxidase. *Arch Biochem Biophys* 70: 150-156, 1957.
31. George J: Role of urate, xanthine oxidase and the effects of allopurinol in vascular oxidative stress. *Vasc Health Risk Manag* 5: 265-272, 2009.
32. Herlitz LC, D'Agati VD and Markowitz GS: Crystalline nephropathies. *Arch Pathol Lab Med* 136: 713-720, 2012.
33. Yang Q, Su S, Luo N and Cao G: Adenine-induced animal model of chronic kidney disease: Current applications and future perspectives. *Ren Fail* 46: 2336128, 2024.
34. Muñoz LIO: Norma Oficial Mexicana NOM-062-ZOO-1999, especificaciones técnicas para la producción, cuidado y uso de los animales de laboratorio., 2001.
35. National Research Council (US) Committee for the Update of the Guide for the Care and Use of Laboratory Animals: Guide for the Care and Use of Laboratory Animals. 8th edition. National Academies Press (US), Washington (DC), 2011.
36. Center For Drug Evaluation and Research: APPLICATION NUMBER: 21-073/S023., 2004.
37. Peng XH, Liang PY, Ou SJ and Zu XB: Protective effect of pioglitazone on kidney injury in diabetic rats. *Asian Pac J Trop Med* 7: 819-822, 2014.
38. Afraz S, Kamran A, Moazzami K, Nezami BG and Dehpour AR: Protective effect of pharmacologic preconditioning with pioglitazone on random-pattern skin flap in rat is mediated by nitric oxide system. *J Surg Res* 176: 696-700, 2012.
39. Leary S, Pharmaceuticals F, Underwood W, Anthony R, Cartner S, Johnson CL and Patterson-Kane E: AVMA guidelines for the euthanasia of animals: 2020 Edition., 2020.
40. Besseling PJ, Pieters TT, Nguyen ITN, de Bree PM, Willekes N, Dijk AH, Bovée DM, Hoorn EJ, Rookmaaker MB, Gerritsen KG, *et al*: A plasma creatinine- and urea-based equation to estimate glomerular filtration rate in rats. *Am J Physiol Renal Physiol* 320: F518-F524, 2021.
41. Livak KJ and Schmittgen TD: Analysis of relative gene expression data using real-time quantitative PCR and the 2(-Delta Delta C(T)) method. *Methods* 25: 402-408, 2001.
42. Farris AB and Colvin RB: Renal interstitial fibrosis: Mechanisms and evaluation. *Curr Opin Nephrol Hypertens* 21: 289-300, 2012.
43. Budi EH, Schaub JR, Decaris M, Turner S and Derynck R: TGF- $\beta$  as a driver of fibrosis: Physiological roles and therapeutic opportunities. *J Pathol* 254: 358-373, 2021.
44. Nogueira A, Pires MJ and Oliveira PA: Pathophysiological mechanisms of renal fibrosis: A review of animal models and therapeutic strategies. *In Vivo* 31: 1-22, 2017.
45. Singh MP, Sharma C and Kang SC: Morin hydrate attenuates adenine-induced renal fibrosis via targeting cathepsin D signaling. *Int Immunopharmacol* 90: 107234, 2021.
46. Aurelien-Cabezas NS, Paz-Michel BA, Jacinto-Cortes I, Delgado-Enciso OG, Montes-Galindo DA, Cabrera-Licona A, Zaizar-Fregoso SA, Paz-Garcia J, Ceja-Espiritu G, Melnikov V, *et al*: Protective effect of neutral electrolyzed saline on Gentamicin-Induced nephrotoxicity: Evaluation of histopathologic parameters in a murine model. *Medicina (Kaunas)* 59: 397, 2023.
47. Zhu CZ, Doyle KJ, Nikkel AL, Olsen L, Namovic MT, Salte K, Widomski D, Su Z, Donnelly-Roberts DL, Gopalakrishnan MM and McGaraghty S: Short-term oral gavage administration of adenine induces a model of fibrotic kidney disease in rats. *J Pharmacol Toxicol Methods* 94: 34-43, 2018.
48. Poulsen HE, Weimann A, Henriksen T, Kjær LK, Larsen EL, Carlsson ER, Christensen CK, Brandslund I and Fenger M: Oxidatively generated modifications to nucleic acids in vivo: Measurement in urine and plasma. *Free Radic Biol Med* 145: 336-341, 2019.
49. Weiner ID, Mitch WE and Sands JM: Urea and ammonia metabolism and the control of renal nitrogen excretion. *Clin J Am Soc Nephrol* 10: 1444-1458, 2015.
50. Kvandova M, Barancik M, Balis P, Puzserova A, Majzunova M and Dovinova I: The peroxisome proliferator-activated receptor gamma agonist pioglitazone improves nitric oxide availability, renin-angiotensin system and aberrant redox regulation in the kidney of pre-hypertensive rats. *J Physiol Pharmacol*: 69, 2018 doi: 10.26402/jpp.2018.2.09. Epub 2018 Jul 4.
51. Asplin JR and Goldfarb DS: Effect of thiazolidinedione therapy on the risk of uric acid stones. *Kidney Int* 95: 1022-1024, 2019.
52. Maalouf NM, Poindexter JR, Adams-Huet B, Moe OW and Sakhaee K: Increased production and reduced urinary buffering of acid in uric acid stone formers is ameliorated by pioglitazone. *Kidney Int* 95: 1262-1268, 2019.
53. Freudlsperger C, Bian Y, Contag Wise S, Burnett J, Coupar J, Yang X, Chen Z and Van Waes C: TGF- $\beta$  and NF- $\kappa$ B signal pathway cross-talk is mediated through TAK1 and SMAD7 in a subset of head and neck cancers. *Oncogene* 32: 1549-1559, 2013.
54. Ni XX, Li XY, Wang Q and Hua J: Regulation of peroxisome proliferator-activated receptor-gamma activity affects the hepatic stellate cell activation and the progression of NASH via TGF- $\beta$ 1/Smad signaling pathway. *J Physiol Biochem* 77: 35-45, 2021.
55. Zhang L, Xu C, Hu W, Wu P, Qin C and Zhang J: Anti-inflammatory effects of Lefty-1 in renal tubulointerstitial inflammation via regulation of the NF- $\kappa$ B pathway. *Int J Mol Med* 41: 1293-1304, 2018.
56. Hou Y, Moreau F and Chadee K: PPAR $\gamma$  is an E3 ligase that induces the degradation of NF $\kappa$ B/p65. *Nat Commun* 3: 1300, 2012.
57. Zhang HB, Zhang Y, Chen C, Li YQ, Ma C and Wang ZJ: Pioglitazone inhibits advanced glycation end product-induced matrix metalloproteinases and apoptosis by suppressing the activation of MAPK and NF- $\kappa$ B. *Apoptosis* 21: 1082-1093, 2016.
58. Sun L, Yuan Q, Xu T, Yao L, Feng J, Ma J, Wang L, Lu C and Wang D: Pioglitazone, a peroxisome proliferator-activated receptor  $\gamma$  agonist, ameliorates chronic kidney disease by enhancing antioxidative capacity and attenuating angiogenesis in the kidney of a 5/6 nephrectomized rat model. *Cell Physiol Biochem* 38: 1831-1840, 2016.
59. Miyamae Y: Insights into dynamic mechanism of ligand binding to peroxisome proliferator-activated receptor  $\gamma$  toward potential pharmacological applications. *Biol Pharm Bull* 44: 1185-1195, 2021.

